Melting of LiF and NaCl to 1 Mbar: Systematics of Ionic Solids at Extreme Conditions

Reinhard Boehler,[1] Marvin Ross,[1,2] and David B. Boercker[2]
[1]*Max-Planck-Institut für Chemie, Postfach 3060, 55020 Mainz, Germany*
[2]*Lawrence Livermore National Laboratory, University of California, Livermore, California 94551*
(Received 17 December 1996)

We report the first diamond cell data for the melting curves of LiF and NaCl up to 1 Mbar (100 GPa). The melting curve of NaCl is in agreement with shock data and shows a break in slope at 290 kbar due to the $B1$(NaCl)-$B2$(CsCl) transition. LiF remains $B1$ to the highest pressure, and molecular dynamic simulations predict that molten LiF retains a simple-cubic $B1$-like structure. A plot of the recent Mainz diamond anvil melting curves for MgO, LiF, KBr, KCl, CsI, and NaCl shows that at very high pressure all the melting curves have very similar slopes approaching a value of order 1–2 K/kbar. [S0031-9007(97)03379-6]

PACS numbers: 62.50.+p, 64.70.Dv

In this paper we report new experimental measurements for the melting curves of LiF and NaCl to pressures up to 1 Mbar and temperatures of the order of 3500 K. These measurements extend the pressure range of previous measurements by over an order of magnitude. Of particular interest is the melt structure of LiF which remains $B1$ to at least 1 Mbar. Although there is an increasing consensus on the experimental determination of melting temperatures from laser heating in a diamond cell [1–7], there is still a debate about the large differences in the melting temperatures of MgO between experiment [8] and molecular dynamics calculations [9–11]. In contrast to most previous materials which have low compressibility, alkali halides can be studied over a much larger compression range, undergo phase transitions at relatively low pressures, and knowledge about their thermodynamic properties makes them more accessible to theoretical studies. In particular, the study of pressure-induced structural changes in melts is important for providing a better understanding of the pressure dependence of melting. In alkali halides the melting curves show a decreasing slope (dT/dP) at high pressure, suggesting the possibility that the density of the melt is nearing that of the solid. Recently, a pressure-induced increase in coordination number in the melt has been confirmed experimentally by x-ray diffraction of molten KBr [12]. This is similar to observations on silicates, based on the pressure-induced coordination change in quenched glasses [13]. In the case of CsI recent melting curve measurements to very high compression and molecular dynamic simulations [14] show that the melt structure changes continuously with increasing pressure from an open structure, similar to a $B1$ melt, to one in which at the highest pressure each ion is surrounded by 10–12 nearest neighbors of mixed charge.

The experimental method employed for measuring melting curves was almost the same as described in the earlier report [14]. Tungsten or rhenium in the form of compressed powder or foil embedded in the sample was heated with a YLF laser in the diamond cell. The samples were of at least 99.99% purity and water was removed in a vacuum furnace at 100 °C before pressure was applied. We used for the first time gaskets made from diamond powder in order to increase the height-to-diameter ratio of the pressure chamber and thus to minimize the thermal conduction from the heated sample to the diamond anvils. Steel gaskets of inner diameter that equals the culet diameter (here 300 μm) were filled with a mixture of 1 μm grain size diamond powder and a small amount of epoxy. After curing, the gasket hole (150 μm diameter) was drilled with conventional tungsten carbide drills. This arrangement proved to be far superior to conventional metal gaskets.

The samples in their solid state did not absorb the laser radiation nor emit incandescent light in detectable amounts throughout the pressure range studied here. As soon as the metal surface reached the melting temperature of the sample, a thin layer in contact with the metal started to melt, resulting in an increase in absorption. The melting temperature was determined by (1) the discontinuous change in the absorption of the laser radiation and (2) by the observation of motion which could be easily observed using the interference pattern created on the metal surface by blue or green laser radiation (Ar or He-Ne laser) [15]. Both methods yielded identical results. For all materials studied so far using this method, the melting temperatures and the slope of the melting curve at low pressures are in perfect agreement with those obtained in a piston cylinder apparatus using thermocouples and differential thermal analysis (DTA) technique (see Figs. 1 and 2).

The data are listed in Table I and are plotted in Figs. 1 and 2. At ambient conditions solid NaCl and LiF are stable in the $B1$ lattice. At 290 kbar NaCl goes to a $B2$ structure. LiF shows no indication of a transition to the highest pressure studied here (1.0 Mbar) or in shock wave experiments to 1 Mbar. The NaCl melting data in Fig. 1 are in excellent agreement with the previous results of Akella [16] up to 65 kbar using a piston cylinder apparatus and DTA. Also shown are the shock temperatures reported by Kormer [17], who

TABLE I. Melting temperatures of NaCl, LiF, and NaF measured in the laser-heated diamond cell.

NaF		LiF		NaCl	
P (kbar)	T_m (K)	P (kbar)	T_m (K)	P (kbar)	T_m (K)
0	1266	0	1118 ± 0	0	1074
220	1968 ± 40	83	1821 ± 70	37	1630 ± 30
233	2041 ± 40	226	2235 ± 70	70,5	1812 ± 50
302	2087 ± 100	385	2693 ± 30	106	1914 ± 50
409	2778 ± 110	475	2734 ± 100	151	1992 ± 62
		609	2920 ± 150	187	2057 ± 100
		785	3098 ± 200	213	2091 ± 120
		885	3072 ± 200	256	2202 ± 110
		927	3108 ± 100	290	2272 ± 100
		1013	3304 ± 190	313	2384 ± 50
				370	2680 ± 50
				410	2935 ± 60
				470	3057 ± 90
				524	3079 ± 80
				592	3202 ± 80
				650	3322 ± 90
				703	3291 ± 90
				775	3350 ± 120
				825	3408 ± 120
				843	3464 ± 130
				911	3525 ± 100

used single wavelength pyrometry for the measurements. Shock temperature measurements by Ahrens *et al.* [18] taken of the melt are in agreement with Kormer. Also shown in Fig. 1 are several points for NaF, showing a similar melting behavior as NaCl. The diamond-cell results for LiF in Fig. 2 are in excellent agreement with the previous measurements of Jackson [19] up to 35 kbar and with molecular dynamics simulations described below, but are in serious disagreement with the shock melting measurement of Kormer [17].

The melting curve of LiF was calculated by the method of constant pressure molecular dynamic (MD) simulations

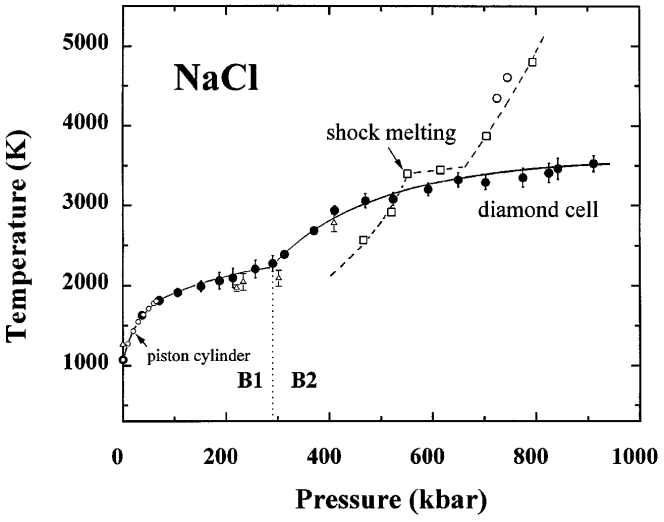

FIG. 1. Diamond cell measurements of the NaCl melting curve. Solid circles (●) are from the present study. Small open circles (o) are the piston-cylinder measurements to 65 kbar of Akella *et al.* [16]. Open squares (□) and large open circles (○) are the shock temperature measurements of Kormer [17] and of Ahrens *et al.* [18], respectively. Open triangles (△) are NaF melting points from the present study.

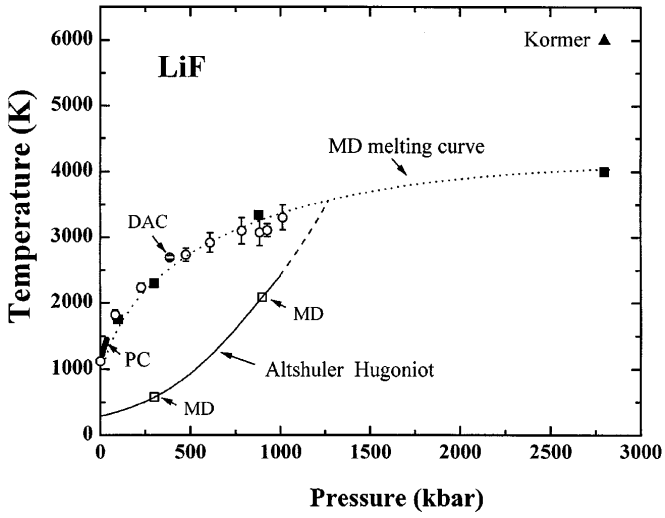

FIG. 2. Melting curve of LiF from diamond cell measurements (○) and molecular dynamics simulations (■). Piston-cylinder measurements (PC) to 35 kbar are from Jackson [19]. The solid line gives the Hugoniot pressures with calculated temperatures of Altshuler *et al.* [22], and the dashed line gives the extrapolated values. (□) Points at which MD simulations were made along the Hugoniot and discussed in text. Shock melting point from Kormer [17] (▲).

using the computer program described previously [14]. In the present study we used 216 particles, and runs were typically two hundred picoseconds. The Tosi-Fumi model [20] was employed for the inter-ion potentials using the functional form and parameters listed by Lewis *et al.* [21]. The model parameters had been fitted to predict the density and bulk modulus at atmospheric pressure and room temperature. Since there are no measurements of the LiF isotherm to 1 Mbar with which to test our potential we made MD calculations of the density at several temperatures and pressures along the Hugoniot to compare with the densities reported by Altshuler *et al.* [22]. Calculations agree exactly with Altshuler's reported density at 300 kbar and 580 K and yield a 2.5% higher density at 900 kbar and 2080 K.

In an earlier study [14] constant pressure MD simulations were made for the enthalpy and volume of the solid and liquid as a function of temperature over a wide range of pressures. These results were then used to calculate the change in volume, ΔV, and change in enthalpy, ΔH, of melting at each pressure. The melting temperatures were then calculated by integrating the Clapeyron equation. In the case of LiF, simulations lead to values of ΔV and ΔH with too much scatter to permit an accurate integration of the Clapeyron equation over the full pressure range as we did with CsI. This scatter lead to an uncertainty of $\pm 10\%$ in the melting temperature at 1 Mbar, which we found unacceptable. However, we did find that the temperature at which the solid became unstable at a given pressure was well defined and predicted a melting curve in excellent agreement with experiment, as shown in Fig. 2. Instability is defined as a discontinuity in the volume and enthalpy. The experience of other researchers for $B1$ melting who employed this method, as summarized by Vocadlo and Price [11], suggests the accuracy of this method is ± 100 K. Also shown in Fig. 2 is the melting point determined along the Hugoniot by Kormer [17]. Our calculations are in considerable disagreement with his measurement. Kormer's result also appears to be in disagreement with Altshuler's Hugoniot measurement and calculated temperatures which predict that the Hugoniot should cross the melting curve near 1.2 Mbar.

In comparison to CsI which transforms from an ordered solid to a partially disordered fluid, LiF transforms from an ordered solid to a nearly ordered melt and therefore undergoes a smaller change in entropy. This is illustrate by the liquid pair distribution functions calculated at 100 kbar for Li^+-F^-, F^--F^-, and Li^+-Li^+, and plotted for the solid in Fig. 3. The first (like-unlike ions) and second (like-like ions) peaks of the liquid are in the same position as the solid but the liquid peaks are slightly shorter and broader. The structural similarity of the solid and liquid diminishes in the third and higher neighbors. In the case of CsI there is considerable mixing between the first and second shells, hence a larger change in entropy. For example, at $T = 3000$ K we found that $\Delta H/k_B T = \Delta S/k_B = 0.7$ for LiF and 2.7 for CsI, where k_B is the Boltzmann constant. The smaller entropy change, by nearly a factor of 4, leads to larger scatter and loss of precision due to an increase in fluctuations between the solid and liquid states. The structural differences between LiF and CsI melts are principally due to the size ratios of their ions which favor charge ordering for LiF.

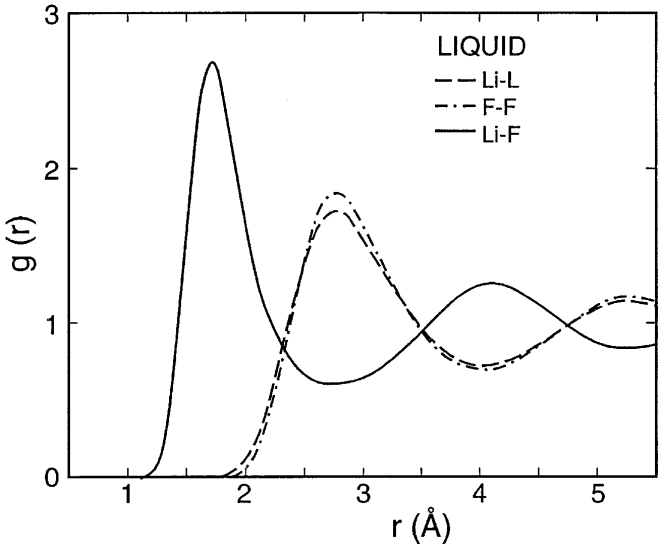

FIG. 3. Radial distribution functions $g(r)$, calculated for liquid LiF near its melting point at 100 kbar.

Plotted in Fig. 4 are the data for all of the very high pressure melting curves for ionic solids measured in this laboratory. The striking feature is that despite the large differences in the initial melting slopes, all the slopes approach nearly the same limiting low value at high pressure. NaCl follows the same pattern even

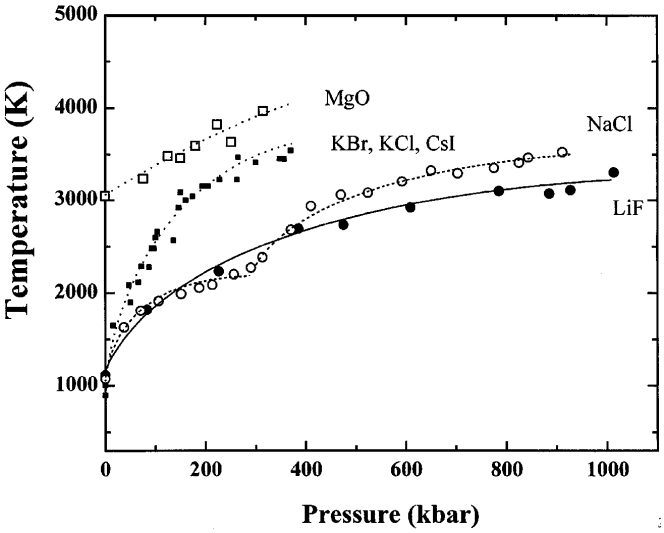

FIG. 4. Summary of very high pressure melting data of ionic solids. MgO from Zerr and Boehler [8]. KCl, KBr, and CsI from Boehler *et al.* [14], and LiF, NaCl from the present report.

though there is a sharp increase in slope above the $B1$-$B2$ transition at 290 kbar. In this regard it is interesting to make some comparisons between LiF and CsI. LiF is exclusively $B1$. CsI is $B2$, showing a splitting of x-ray diffraction lines above 150 kbar which, however, below 450 kbar is too small to permit an identification of the orthorhombic structure [23]. Our previous melting data on CsI were taken up to 265 kbar, and we saw no indication of a structural change both in the experiment (as we see, for example, for NaCl) and in the calculations. Therefore LiF and CsI may be considered prototypical materials for their structures. At 300 kbar the enthalpy change at melting of CsI is nearly a factor of 4 larger than for LiF. Although the fractional volume changes of both materials are only a few percent, the volume of LiF is approximately a factor of 4 smaller and consequently its ΔV is also a factor of 4 smaller. As a result both materials have similar ratios of $\Delta V/\Delta H$ at high pressure and therefore similar melting slopes.

At high pressure the melting slopes of the alkali halides approach that measured for MgO [8]. MgO in solid solution with some FeO is an important component of the Earth's lower mantle, and it has been shown that the melting behavior of MgO is very similar to the iron containing lower mantle component [8]. These measurements are in considerable disagreement with recent MD simulations [10,11] which predict a melt slope, dT/dP, about three times larger. Unfortunately, the JANAF tables [24] cite values for ΔH for MgO at 1 bar that vary by a factor of 4 and no experimental estimates of ΔV are available, which prohibits a direct calculation of the initial melting slope. An argument supporting the measured melting slope for MgO may be made by a comparison of LiF at high pressure with MgO. LiF and MgO are isoelectronic materials, have nearly the same ion radius-ratios, retain the $B1$ structure over a large pressure range, and as in the present molecular dynamics simulation for LiF, the structures of solid and liquid MgO become increasingly alike at high pressure, resulting in a limiting slope at very high pressure [11,25]. At high pressure both materials have spheres of nearly the same size in terms of a charged hard sphere model, thus, both should have similar values of ΔV and the entropy change of melting ΔS, and therefore should have similar melting slopes.

In summary, the results presented here cover the largest compression range (50%) over which melting has thus far been measured. The melting slopes for all the binary ionic solids studied to date suggest a limiting value of 1–2 K/kbar at very high pressure. It is interesting that this was also observed for other classes of materials such as for some metals at very high pressure [2,26], and for MgO [8,10] in spite of the large differences in their initial melting slopes. Even measurements of argon suggest such a trend [3,27]. If this melting behavior at very high pressure is applied to silicates, it may have important ramifications for geophysics.

[1] R. Boehler, Annu. Rev. Earth Planet. Sci. **24**, 15–40 (1996).
[2] R. Boehler, Nature (London) **363**, 534–536 (1993).
[3] A. P. Jephcoat and S. P. Besedin, Philos. Trans. R. Soc. London A **354**, 1333–1360 (1996).
[4] S. K. Saxena, G. Shen, and P. Lazor, Science **264**, 405–407 (1994).
[5] C. S. Yoo, J. Akella, and C. Ruddle, EOS Trans. Am. Geophys. Union **73**, 64 (1992).
[6] C. S. Yoo *et al.*, Science **270**, 1473–1475 (1995).
[7] G. Shen and P. Lazor, J. Geophys. Res. **100**, 17 699–17 713 (1995).
[8] A. Zerr and R. Boehler, Nature (London) **371**, 506–508 (1994).
[9] Z. Gong, R. E. Cohen, and L. L. Boyer, in *Annual Report of the Director of the Geophysical Laboratory* (Carnegie Institution, Washington, DC, 1991), Vols. 1990–1991, pp. 129–134.
[10] R. E. Cohen and Z. Gong, Phys. Rev. B **50**, 12 301–12 311 (1994).
[11] L. Vocadlo and G. D. Price, Phys. Chem. Miner. **23**, 42–49 (1996).
[12] S. Urakawa *et al.*, High Press. Res. **14**, 375 (1996).
[13] E. M. Stolper and T. J. Ahrens, Geophys. Res. Lett. **14**, 1231–1233 (1987).
[14] R. Boehler, M. Ross, and D. B. Boercker, Phys. Rev. B **53**, 556–563 (1996).
[15] R. Boehler, Phys. Earth Planet. Inter. **96**, 181–186 (1996).
[16] J. Akella, S. N. Vaidya, and G. C. Kennedy, Phys. Rev. **185**, 1135–1140 (1969).
[17] S. B. Kormer, Sov. Phys. Usp. **11**, 229–254 (1968).
[18] T. J. Ahrens, G. A. Lyzenga, and A. C. Mitchell, in *Advances in Earth and Planetary Sciences*, edited by S. Akimoto and M. H. Manghnani (Center of Academic Publications, Tokyo, 1982).
[19] I. Jackson, Phys. Earth Planet. Inter. **14**, 86–94 (1977).
[20] M. P. Tosi and F. C. Fumi, J. Phys. Chem. Solids **25**, 31 (1964).
[21] J. W. E. Lewis, K. Singer, and L. V. Woodcock, Trans. Faraday Soc. **71**, 301 (1975).
[22] L. V. Altshuler *et al.*, Sov. Phys. Solid State **5**, 203–211 (1963).
[23] H. K. Mao *et al.*, Phys. Rev. Lett. **64**, 1749–1752 (1990).
[24] *JANAF Thermochemical Tables* (U.S. National Bureau of Standards, Washington, DC, 1971), 2nd ed., p. 1141.
[25] A. B. Belonoshko and L. S. Dubrovinsky, Am. Mineral. **81**, 303–316 (1996).
[26] R. Boehler and M. Ross (to be published).
[27] C. S. Zha *et al.*, J. Chem. Phys. **85**, 1034–1036 (1986).